

bullous disease, pneumatocele, Swyer-James syndrome, endobronchial mass, unilateral pulmonary agenesis, proximal interruption of the pulmonary artery, scimitar syndrome, diaphragmatic hernia, and Poland syndrome<sup>(8)</sup>. It can also include an intrathoracic mass or vascular ring. HRCT is useful for confirming radiographic findings, delineating the affected lobe and showing relative narrowing of the bronchus associated with hyperinflation and attenuated vessels in the hyperlucent lobe, which facilitate the differential diagnosis.

Lobectomy is the treatment for nearly all cases of CLE with respiratory distress. According to Karnak et al.<sup>(10)</sup>, lobectomy is the recommended treatment for CLE in all infants under two months of age and in older infants who present with severe respiratory symptoms. Apparently, the earlier the presentation is, the greater is the need for surgery. Conservative management, with close outpatient follow-up, can be used in older children who present with mild to moderate symptoms. Because our patient had remained asymptomatic throughout her life, her case was managed with clinical and radiographic follow-up.

REFERENCES

1. Werner Jr H, Santos JL, Belmonte S, et al. Applicability of three-dimensional imaging techniques in fetal medicine. *Radiol Bras.* 2016;49:281-7.
2. Barbosa AGJ, Penha D, Zanetti G, et al. Foreign body in the bronchus of a child: the importance of making the correct diagnosis. *Radiol Bras.* 2016;49:340-2.

3. Vilela VM, Ribeiro VM, Paiva JC, et al. Clinical and radiological characterization of fibrous hamartoma of infancy. *Radiol Bras.* 2017;50:204-5.
4. Figueiras FN, Duarte ML, Duarte ER, et al. Giant ovarian teratoma: an important differential diagnosis of pelvic masses in children. *Radiol Bras.* 2017;50:342-3.
5. Schiavon JLO, Caran EMM, Odone Filho V, et al. The value of anterior displacement of the abdominal aorta in diagnosing neuroblastoma in children. *Radiol Bras.* 2016;49:369-75.
6. Sodhi KS, Bhatia A, Khandelwal N. Rapid MRI of the lungs in children with pulmonary infections. *Radiol Bras.* 2016;49:126.
7. Cataneo DC, Rodrigues OR, Hasimoto EN, et al. Congenital lobar emphysema: 30-year case series in two university hospitals. *J Bras Pneumol.* 2013;39:418-26.
8. Dillman JR, Sanchez R, Ladino-Torres MF, et al. Expanding upon the unilateral hyperlucent hemithorax in children. *Radiographics.* 2011;31:723-41.
9. Kumar B, Agrawal LD, Sharma SB. Congenital bronchopulmonary malformations: a single-center experience and a review of literature. *Ann Thorac Med.* 2008;3:135-9.
10. Karnak I, Senocak ME, Ciftci AO, et al. Congenital lobar emphysema: diagnostic and therapeutic considerations. *J Pediatr Surg.* 1999;34:1347-51.

Felipe Mussi von Ranke<sup>1</sup>, Heloisa Maria Pereira Freitas<sup>2</sup>, Vanessa Dinoá<sup>1</sup>, Fernanda Miraldi<sup>1</sup>, Edson Marchiori<sup>1</sup>

1. Universidade Federal do Rio de Janeiro (UFRJ), Rio de Janeiro, RJ, Brazil. Mailing address: Dr. Edson Marchiori. Rua Thomaz Cameron, 438, Valparaíso, Petrópolis, RJ, Brazil, 25685-120. E-mail: edmarchiori@gmail.com.

<http://dx.doi.org/10.1590/0100-3984.2016.0224>

Erdheim-Chester disease with isolated neurological involvement

Dear Editor,

A 25-year-old female patient presented with a seven-month history of progressive dysphagia, dysphonia, diplopia, ptosis of the right eyelid, weight loss, and sporadic pulsatile headache on the right side of the face. She had a history of hypertension, diabetes, unspecified thyroid disease, and smoking. The physical examination revealed satisfactory general health, although the patient was found to be malnourished, as well as to have deficits in the right third, fifth, and sixth cranial nerves. Magnetic resonance imaging (Figure 1) showed an expansile lesion located in the right sellar and juxtaseilar region. A transsphenoidal biopsy was performed. The pathology and immunohistochemical study showed xanthomatous macrophages, together with CD 68 posi-

tive and CD1A negative histiocytes, consistent with a diagnosis of Erdheim-Chester disease. Computed tomography of the chest and abdomen showed no abnormalities.

Erdheim Chester disease is currently considered a clonal disorder, the pathogenesis of which is mediated primarily by a chronic, uncontrolled inflammatory process<sup>(1)</sup>. The Th1-type immune response involves activation of the following cytokines: IFN- $\gamma$ , IL-1/IL-1Ra, IL-6, IL-12, and MCP-1/CCL2. In studies of Erdheim-Chester disease, the most commonly reported gene mutation is that occurring in the BRAF V600E gene, which is seen in 57-75% of patients diagnosed with the disease. Mutations have also been reported in the MAPK (NRAS and MAP2K1) and PIK3 (PIK3CA) pathways<sup>(2)</sup>.

Histopathologically, Erdheim-Chester disease is a non-Langerhans cell histiocytosis, characterized by numerous macro-

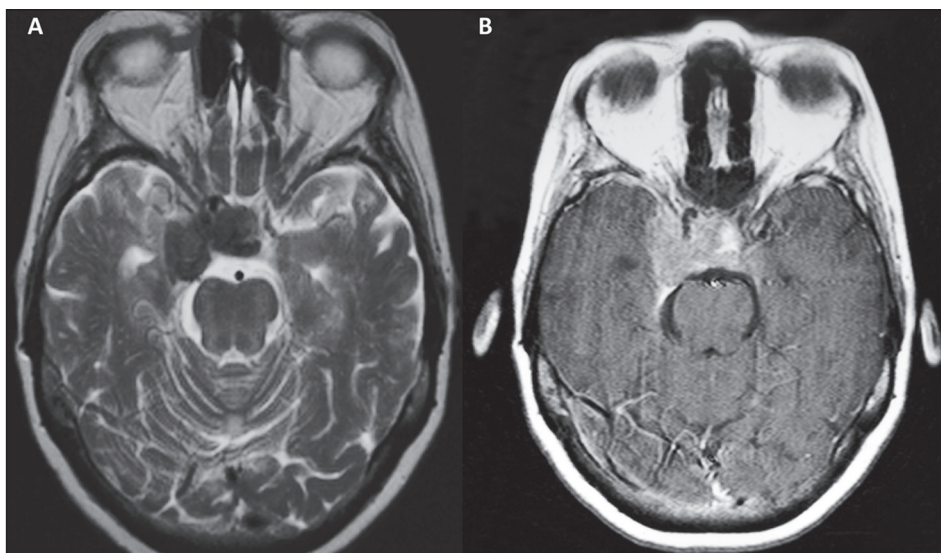
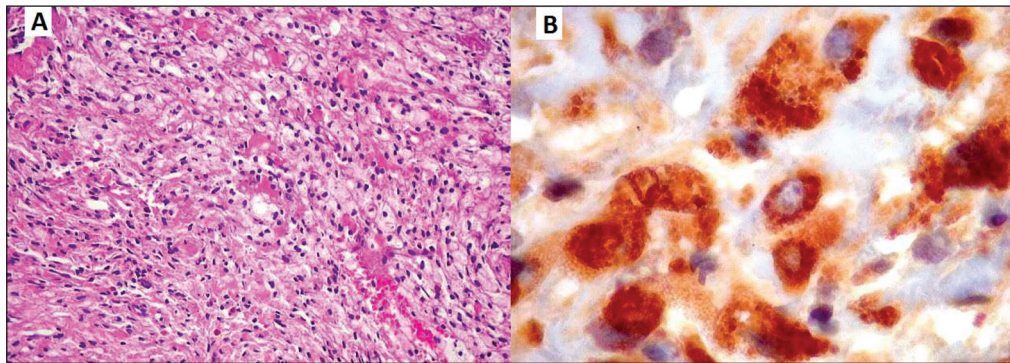


**Figure 1.** Magnetic resonance imaging scan showing a well-defined, compact, lobulated expansile lesion, measuring 3.0 × 1.5 × 3.0 cm, located in the right sellar and juxtaseilar region, invading and occupying the sella turcica and the right juxtaseilar region, with a hypointense signal on a T2-weighted image (A) and intense enhancement on a T1-weighted image acquired after gadolinium contrast administration (B). Note the reduction in the caliber of the intracavernous carotid arteries. The lesion is compressing and displacing the optic chiasm anteriorly, cavitating the right medial temporal region, surrounding the pituitary gland, and extending to the supra-sellar cistern. Anteriorly, it reaches the right optic canal.

**Figure 2.** Non-Langerhans cell histiocytosis of the skull base. **A:** Photomicrograph showing abundant xanthomatous macrophages, in a solid arrangement, with small, dense nuclei and clear cytoplasm with lipid droplets. The cytoplasmic boundaries were more or less defined, depending on the area. **B:** Photomicrograph showing positivity for the macrophage marker CD68, which was the main antigen demonstrated in the lesion.



phages with xanthomatous cytoplasm and small nuclei, together with giant cells, as well as few lymphocytes and eosinophils. The histiocytes are positive for CD-68, negative for S-100 protein, and negative for CD1A. It is noteworthy that Langerhans cells are positive for CD1A, negativity for CD1A therefore ruling out a diagnosis of Langerhans cell histiocytosis<sup>(3)</sup>.

Clinically, Erdheim-Chester disease manifests as a systemic disease, involving bone, as well as the central nervous system (CNS), eyes, lungs, mediastinum, kidneys, and retroperitoneum<sup>(4)</sup>. The most common symptoms are bone pain accompanied by progressive weakness, especially in the lower limbs, together with fever, weight loss, exophthalmos, dyspnea, and signs of neurological impairment such as diabetes insipidus.

A recent extensive systematic review of 331 articles, including a collective total of 448 patients diagnosed with Erdheim-Chester disease, showed that neurological involvement was present as an initial manifestation in 25% of the patients and over the course of the disease in 50%<sup>(5)</sup>. Exophthalmos, other eye disorders, diabetes insipidus, cerebellar syndromes, seizure, and radiculopathy were the most commonly observed CNS manifestations. The most common features seen on imaging examinations were retro-orbital masses, involvement of the cerebellar dentate nucleus and meningeal lesions of the dura mater, as well as areas of cerebellar and brain stem demyelination. Suprasellar and infundibular lesions were more often accompanied by diabetes insipidus, hypopituita-

rism, and hyperprolactinemia. Involvement of the spinal cord was less common than was involvement of the brain and brain stem<sup>(5)</sup>.

In the present case, the neurological impairment was isolated. In the literature, we found no other reports of exclusive involvement of the CNS. The gender and age of our patient were also uncommon, given that the prevalence of Erdheim-Chester disease is highest among male patients between the 5th and the 7th decades of life<sup>(5)</sup>.

#### REFERENCES

1. Diamond EL, Dagna L, Hyman DM, et al. Consensus guidelines for the diagnosis and clinical management of Erdheim-Chester disease. *Blood*. 2014; 124:483–92.
2. Haroche J, Papo M, Cohen-Aubart F, et al. Erdheim-Chester disease (ECD), an inflammatory myeloid neoplasia. *Presse Med*. 2017;46:96–106.
3. Johnson MD, Aulino JP, Jagasia M, et al. Erdheim-Chester disease mimicking multiple meningiomas syndrome. *AJNR Am J Neuroradiol*. 2004;25:134–7.
4. Hessel FF, Canazaro LF, Capoani M, et al. Erdheim-Chester disease: a two-case report. *Radiol Bras*. 2009;42:267–9.
5. Cives M, Simone V, Rizzo FM, et al. Erdheim-Chester disease: a systematic review. *Crit Rev Oncol Hematol*. 2015;95:1–11.

**Bruna Melo Coelho Loureiro<sup>1</sup>, Albina Messias Altemani<sup>1</sup>, Fabiano Reis<sup>1</sup>**

1. Universidade Estadual de Campinas (Unicamp), Campinas, SP, Brazil. Mailing address: Dra. Bruna Melo Coelho Loureiro. Universidade Estadual de Campinas – Radiologia. Rua Tessália Vieira de Camargo, 126, Cidade Universitária Zeferino Vaz. Campinas, SP, Brazil, 13083-887. E-mail: bruna\_mcl@hotmail.com.

<http://dx.doi.org/10.1590/0100-3984.2016.0218>

#### **Pseudocyst in ectopic pancreas: diagnosis and percutaneous treatment guided by MDCT**

Dear Editor,

A 40-year-old man presented with a 12-h history of severe abdominal pain, nausea, and vomiting. Although he reported no comorbidities, he stated that he had concomitant constipation and had consumed alcoholic beverages over the past three days. Physical examination revealed pain on palpation of the lower abdomen. Multidetector computed tomography (MDCT) of the abdomen showed a normal pancreas and tissue formation with a density of 30 HU, similar to that of the pancreatic parenchyma (Figure 1), located in the mesentery, in close contact with the proximal segment of the jejunal loop, measuring 2.8 × 2.9 × 2.9 cm, with adjacent liquid (Figures 1 and 2). The patient was hospitalized, with high levels of amylase and lipase, being treated with nutritional support and antibiotic coverage. His pain worsened, persisting for 12 more days. Another MDCT scan showed the formation of a pseudocapsule, with contrast enhancement and residual adjacent fluid. To look for infection, we opted for percutaneous drainage, smear cytology, and determination of

the amylase level in the liquid (Figure 2). Cytometry showed the presence of leukocytes, a differential count with a predominance of mononuclear cells (60% lymphocytes), and the absence of malignancy. The Gram stain was negative, as were tests for fungi, acid-fast bacilli, and other bacteria. The pH was 7.79, the LDH level was 405 IU/mL, and the amylase level was 1207 IU/L. The post-drainage evolution was favorable, and the patient was discharged in good clinical condition. At this writing, he has been in outpatient follow-up for six months, during which time he has been asymptomatic.

Tumors and pseudotumors of the upper abdomen have been the subject of recent studies in the radiology literature of Brazil<sup>(1–7)</sup>. Ectopic pancreas is a rare condition that is most common in males between the fourth and sixth decades of life. It is defined as pancreatic tissue in an anomalous location, with no anatomical, neural, or vascular connection with the normal pancreas<sup>(8)</sup>. Although the pathogenesis of ectopic pancreas is unknown, there are two hypotheses: the first suggests that there is transplantation of embryonic pancreatic cells to neighboring structures during the intestinal rotation process; and the second proposes that embryonic buds remain attached to the primitive